

A non-perturbative study of the action parameters for anisotropic-lattice quarks

Justin Foley,¹ Alan Ó Cais,¹ Mike Peardon,¹ and Sinéad M. Ryan¹

(TrinLat Collaboration)

¹*School of Mathematics, Trinity College, Dublin 2, Ireland*

(Dated: November 21, 2018)

A quark action designed for highly anisotropic lattice simulations is discussed. The mass-dependence of the parameters in the action is studied and the results are presented. Applications of this action in studies of heavy quark quantities are described and results are presented from simulations at an anisotropy of six, for a range of quark masses from strange to bottom.

I. INTRODUCTION

The anisotropic lattice has proved an invaluable tool for simulations of a variety of physical quantities. The precision calculation of the glueball spectrum was an early application of the approach [1] and it was recognised that anisotropic actions may also be advantageous in heavy quark physics calculations [2]. Correlators of heavy particles such as glueballs and hadrons with a charm or bottom quark have a signal which decays rapidly. Monte Carlo estimates of these correlation functions can be noisy, making it difficult to resolve a plateau over a convincing range of lattice time steps. Increasing the number of timeslices for which the effective mass of a particle has reached a plateau solves this problem and also decreases the statistical error in the fitted mass. Since this value may be used as an input to determine many physical parameters this decrease is very beneficial.

Secondly, improved precision in effective mass fits means that momentum-dependent errors of $\mathcal{O}(ap)$ can be disentangled from other discretisation effects and larger particle momenta may be considered. This is particularly relevant for the determination of semileptonic decay form factors where the overlap of momentum regions accessible to experiments and lattice calculations is currently very small. Typically, experiments have more events with daughter particle momentum at or above 1 GeV. This is also the region where large momentum-dependent errors are expected in lattice calculations. The form factors of decays like $B \rightarrow \pi \ell \nu$ and $B \rightarrow K^* \gamma$ are inputs to determinations of CKM parameters so that increased precision in lattice calculations can lead to tighter constraints on the Standard Model. This has motivated a study of 2+2 anisotropic lattices where the temporal and one spatial direction are made fine and all momentum is injected along this fine spatial axis. Details of the progress to date in this work are in Refs. [3] and [4]. The 2+2 formulation has also proved useful for a precision determination of the static interquark potential over large separations, which is described in Ref. [3]. In this paper we consider a 3+1 anisotropic action. The temporal lattice spacing, a_t is made fine relative to the spatial spacing, a_s . The action is designed with simulations at large anisotropies in mind. To simulate a bottom quark with a relativistic action requires a lattice spacing of less than 0.04 fm which is prohibitively expensive on an isotropic lat-

tice where the simulation cost scales at least as $\mathcal{O}(a^{-4})$. The anisotropic lattice offers the possibility of relativistic heavy-quark physics using reasonably modest computing resources. In the rest frame of a hadron with a heavy constituent, the quark four-momentum is closely aligned with the temporal axis, allowing an anisotropic discretisation to represent accurately the Dirac operator on the quark field.

Implementing an anisotropic programme incurs a number of computational overheads not associated with the isotropic lattice. The ratio of scales, $\xi = a_s/a_t$ determined by studying a physical long-distance probe depends on bare parameters in the lattice action. While this dependence is straightforward to establish at the tree-level of perturbation theory, quantum corrections can occur at higher orders. In the quenched approximation on a 3+1 lattice this is not a serious additional cost as the tuning can be done *post-hoc*. More worryingly, in Ref. [5] it was pointed out that the choice of ξ and its relation to the Wilson parameter, r on anisotropic versions of the Sheikholeslami-Wohlert (SW) action could introduce $\mathcal{O}(a_s m_q)$ errors. It is exactly errors of this type that the anisotropic action seeks to avoid and the appearance of these terms represents a serious tuning problem.

In this paper we use an action, specifically designed for highly anisotropic lattices ie. $\xi \geq 5$. By applying different improvement terms in the spatial and temporal directions the action is both doubler and $\mathcal{O}(a_s m_q)$ error free. This opens up the possibility of simulating directly at the bottom quark mass using a relativistic action. In addition, in this feasibility study the speed of light was determined at $\approx 1\%$ accuracy. This precision was governed by finite statistics and could certainly be improved upon.

The paper is organised as follows. The construction of the action is described in Section II. Section III compares this action with the sD34 action proposed in Ref. [6] and details some analytic results. Results from a study of the dispersion relations and the mass-dependence of the speed of light are described in Section IV. Some preliminary results of this study have appeared in Ref. [7]. Our conclusions and a discussion of future work are contained in Section V.

II. DESIGNING HIGHLY ANISOTROPIC ACTIONS

We begin by considering a Wilson-type action with Symanzik improvement to remove discretisation errors. Full $\mathcal{O}(a)$ -improvement requires a clover term and a field rotation, given by

$$\psi = [1 - \frac{ra}{4}(\mathcal{P} - m)]\psi', \quad (1)$$

$$\bar{\psi} = \bar{\psi}'[1 - \frac{ra}{4}(\mathcal{P} - m)], \quad (2)$$

where a is the lattice spacing on an isotropic lattice and r is the usual Wilson parameter. The rotation described by Eqs. (1) and (2) preserves locality and maintains a positive transfer matrix so that ghost states do not arise in a calculation of the free fermion propagator. However, in an anisotropic implementation of this action, when a_t is made very small, these rotations may lead to the reappearance of doublers, an undesirable side-effect of the anisotropy.

We would like to maintain the useful properties of actions with nearest neighbour temporal interactions only. In particular, the positivity of the transfer matrix guarantees that effective masses approach a plateau from above. Therefore, to construct an action suitable for high anisotropies we begin by applying field rotations in the temporal direction only, rewriting Eqs. (1) and (2) as

$$\psi = [1 - \frac{ra_t}{4}(\gamma_0 D_0 - m)]\psi', \quad (3)$$

$$\bar{\psi} = \bar{\psi}'[1 - \frac{ra_t}{4}(\gamma_0 D_0 - m)]. \quad (4)$$

This leads to a new action in which the temporal and spatial directions are treated differently. Having applied the rotations of Eqn. (2) the continuum action is given by

$$S' = \bar{\psi}' M_r \psi' - \frac{ra_t}{2} \bar{\psi}' \left(D_0^2 - \frac{g}{2} \epsilon_i E_i \right) \psi'. \quad (5)$$

where $M_r = \mu_r \gamma_i D_i + \gamma_0 D_0 + \mu_r m$ and $\mu_r = (1 + \frac{1}{2} r a_t m)$. At the tree-level, the rotations described in Eqs. (3) and (4) do not generate a spatial clover term. As a result the $(\sigma \cdot \mathbf{B})$ term does not appear in Eq. (5). The chromoelectric field, E_i is defined as

$$igE_i = [D_i, D_0], \quad (6)$$

and $\epsilon_i \equiv \sigma_{i0}$ is given by $\epsilon_i = \frac{1}{2i}[\gamma_i, \gamma_0]$.

The temporal doublers are removed by discretising the D_0^2 term in the usual way. However, with no spatial rotation the spatial doublers remain and must be treated separately. They are removed by adding a higher-order, irrelevant operator to the action. This was first suggested by Hamber and Wu in Ref. [8]. The simplest such operator is a spatial D^4 term which is added *ad hoc* to the

Dirac operator giving an action,

$$S' = \bar{\psi}' M_r \psi' - \frac{ra_t}{2} \bar{\psi}' \left(D_0^2 - \frac{g}{2} \epsilon_i E_i \right) \psi' + s a_s^3 \bar{\psi}' \sum_i D_i^4 \psi'. \quad (7)$$

This approach has previously been discussed in detail in Ref. [9]. In this formulation, s is a Wilson-like parameter which is chosen such that the doublers receive a sufficiently large mass. The discretisation of the action in Eq. (7) is now straightforward. Only the $\gamma_i D_i$ term requires an improved discretisation since the simplest discretisation would lead to $\mathcal{O}(a_s^2)$ errors. For this case we write

$$\Delta_{imp}^{(1)} \phi(x) = \frac{1}{a} \left\{ \frac{2}{3} [\phi(x+a) - \phi(x-a)] - \frac{1}{12} [\phi(x+2a) - \phi(x-2a)] \right\} \quad (8)$$

and similarly the (unimproved) discretisations of ∂ , ∂^2 and ∂^4 are

$$\Delta^{(1)} \phi(x) = \frac{1}{2a} \{ \phi(x+a) - \phi(x-a) \}, \quad (9)$$

$$\Delta^{(2)} \phi(x) = \frac{1}{a^2} \{ \phi(x+a) + \phi(x-a) - 2\phi \}, \quad (10)$$

$$\Delta^{(4)} \phi(x) = \frac{1}{a^4} \{ [\phi(x+2a) + \phi(x-2a)] - 4[\phi(x+a) - \phi(x-a)] + 6\phi(x) \}. \quad (11)$$

The corresponding gauge covariant derivatives, D , D^2 and D^4 respectively are constructed by including link variables in the usual way. The chromoelectric field is discretised by a clover term with plaquettes in the three space-time planes only

$$gE_i = \frac{1}{\xi a_t^2} \frac{1}{u_s^2 u_t^2} \frac{1}{8i} \left\{ \Omega_i(x) - \Omega_i^\dagger(x) \right\}, \quad (12)$$

with

$$\begin{aligned} \Omega_i(x) = & U_i(x) U_t(x+\hat{i}) U_i^\dagger(x+\hat{i}) U_t^\dagger(x) \\ & + U_t(x) U_i^\dagger(x-\hat{i}+\hat{t}) U_t^\dagger(x-\hat{i}) U_i(x-\hat{i}) \\ & + U_i^\dagger(x-\hat{i}) U_t^\dagger(x-\hat{i}-\hat{t}) U_i(x-\hat{i}-\hat{t}) U_t(x-\hat{t}) \\ & + U_t^\dagger(x-\hat{t}) U_i(x-\hat{t}) U_t(x+\hat{i}-\hat{t}) U_i^\dagger(x). \end{aligned} \quad (13)$$

u_s and u_t are the mean-link improvement parameters. u_s is determined from the spatial plaquette and u_t is set to unity. At the accuracy of the action constructed here no improvement is required. Finally, including the gauge fields and the mean-link improvement factors the lattice fermion matrix is given by,

$$\begin{aligned}
M_{\text{ARIA}}\psi(x) = & \frac{1}{a_t} \left\{ \left(\mu_r m a_t + \frac{18s}{\xi} + r + \frac{r a_t^2 g}{4} \epsilon_i E_i \right) \psi(x) - \frac{1}{2u_t} \left[(r - \gamma_0) U_t(x) \psi(x + \hat{t}) + (r + \gamma_0) U_t^\dagger(x - \hat{t}) \psi(x - \hat{t}) \right] \right. \\
& - \frac{1}{\xi_q} \sum_i \left[\frac{1}{u_s} \left(4s - \frac{2}{3} \mu_r \gamma_i \right) U_i(x) \psi(x + \hat{i}) + \frac{1}{u_s} \left(4s + \frac{2}{3} \mu_r \gamma_i \right) U_i^\dagger(x - \hat{i}) \psi(x - \hat{i}) \right. \\
& \left. \left. - \frac{1}{u_s^2} \left(s - \frac{1}{12} \mu_r \gamma_i \right) U_i(x) U_i(x + \hat{i}) \psi(x + 2\hat{i}) - \frac{1}{u_s^2} \left(s + \frac{1}{12} \mu_r \gamma_i \right) U_i^\dagger(x - \hat{i}) U_i^\dagger(x - 2\hat{i}) \psi(x - 2\hat{i}) \right] \right\}. \quad (14)
\end{aligned}$$

At the tree-level, the fermion anisotropy ξ_q is given by the ratio of scales, $\xi = a_s/a_t$. We call the action described here ARIA for Anisotropic, Rotated, Improved Action. It is classically improved to $\mathcal{O}(a_t, a_s^3)$.

III. HEAVY QUARKS WITH ARIA

The precision calculation of the glueball spectrum on coarse lattices [1] suggests that heavy hadronic quantities would also benefit from the anisotropic formulation. The correlation functions for heavy-heavy and heavy-light mesons fall off rapidly with time and it can be difficult to isolate a convincing plateau over a reasonable number of timeslices. A lattice with fine temporal direction in principle solves this problem by providing a large number of timeslices over which the time-dependence can be resolved. Improved Wilson actions on anisotropic lattices have been used to study a range of heavy flavour physics including charmonium and bottomonium spectroscopy [10, 11, 12], heavy-light and hybrid spectra [13, 14, 15, 16] and also heavy-light semileptonic decays [17].

In these calculations, currents are improved using rotations, which are applied identically in all four space-time directions and the Wilson parameter in the spatial direction is usually chosen to be either $r_s = 1/\xi$ [18, 19] or $r_s = 1 = r_t$ [20, 21, 22, 23]. However, it was pointed out in Ref. [5] that simulations with anisotropic Wilson-type actions may include $\mathcal{O}(a_s m_q)$ effects. Naively, errors of this form are unexpected but they arise in products of the Wilson and mass terms in the action. In particular, the authors showed that the presence of these artefacts, which appear in radiative corrections, depends on the spatial Wilson parameter, r_s . The $\mathcal{O}(a_s m_q)$ -dependence potentially spoils the benefits of working on an anisotropic lattice, especially at large quark masses.

In Ref. [6] a different approach was adopted. Since the unwanted $\mathcal{O}(a_s m_Q)$ -dependent terms arise from the spatial Wilson term the authors propose an anisotropic D234-type action [2] may be more suitable. In this case a rotation term is applied in the temporal direction only, removing the temporal doublers. Spatial doublers are removed by adding an irrelevant, dimension-four term to the Dirac operator. The authors showed to one-loop order in perturbation theory, that this so-called ‘‘sD34’’

action does not suffer from $\mathcal{O}(a_s m_q)$ terms. Comparing the ARIA action proposed in Section II and the sD34 action from Ref. [6] we see that these are the same, up to $\mathcal{O}(a_t)$ improvement.

The D234 quark action on an anisotropic lattice [2] is written

$$S_{D234} = a_t a_s^3 \sum_x \bar{\psi}(x) M \psi(x), \quad (15)$$

and writing M in the notation of Ref. [6]

$$\begin{aligned}
M = & m_0 + \sum_\mu \nu_\mu \gamma_\mu \nabla_\mu (1 - b_\mu a_\mu^2 \Delta_\mu) - \frac{1}{2} a_t \left(\sum_\mu r \Delta_\mu \right. \\
& \left. + \sum_{\mu < \nu} c_{\text{SW}}^\mu \sigma_{\mu\nu} F_{\mu\nu} \right) + \sum_\mu \nu_\mu d_\mu a_\mu^2 \Delta_\mu^2. \quad (16)
\end{aligned}$$

The sD34 action is a special case of this action in which the parameters have the following values

$$\begin{aligned}
(\nu_0, \nu_i) &= (1, \nu); & (b_0, b_i) &= (0, \frac{1}{8}); & (d_0, d_i) &= (0, \frac{1}{8}); \\
(r_0, r_i) &= (r_t, 0); & (c_{\text{SW}}^0, c_{\text{SW}}^i) &= (0, c_{\text{SW}}). \quad (17)
\end{aligned}$$

and $\nu = (1 + \frac{1}{2} r_t a_t m_0)$. Substituting in Eq. (16) gives

$$\begin{aligned}
M_{\text{sD34}} = & m_0 + \sum_i \nu \gamma_i \nabla_i \left(1 - \frac{1}{6} a_s^2 \Delta_i \right) + \gamma_0 \nabla_0 \\
& - \frac{a_t}{2} (r \Delta_0 + c_{\text{SW}}^t \sigma_{i0} F_{i0}) + \frac{1}{8} a_s^3 \sum_i \nu \Delta_i^2, \quad (18)
\end{aligned}$$

which is the action we use in our simulations, up to $\mathcal{O}(a_t)$ improvement. Reexpressing the fermion matrix in our notation,

$$\begin{aligned}
M_{\text{ARIA}} = & \mu_r m_0 + \sum_i \mu_r \gamma_i \nabla_i \left(1 - \frac{1}{6} a_s^2 \Delta_i \right) + \gamma_0 \nabla_0 \\
& - \frac{a_t}{2} \left(r \Delta_0 - \frac{r g}{2} \sigma_{i0} F_{i0} \right) + s a_s^3 \sum_i \Delta_i^2, \quad (19)
\end{aligned}$$

where $s = 1/8$ and $\mu_r = (1 + \frac{1}{2} r_t a_t m_0)$.

A. Analytic results for ARIA

In this section the energy-momentum behaviour of the ARIA action is calculated. We begin by presenting results for general r and s . The free-quark dispersion relation is obtained by solving $\det \widetilde{M}_{\text{ARIA}} = 0$ in momentum

space where $\widetilde{M}_{\text{ARIA}}$ is the Fourier transform of M_{ARIA} in Eq. (14). The energy-momentum relation is

$$\cosh(Ea_t) = \frac{r^2 + r\omega(p)}{r^2 - 1} \pm \frac{\sqrt{(r + \omega(p))^2 + (1 - r^2)(1 + a_t^2 \tilde{\mathbf{p}}^2)}}{r^2 - 1}, \quad (20)$$

where $\omega(p)$ and $\tilde{\mathbf{p}}$ are defined as

$$\omega(p) = a_t \mu_r m_0 + a_t s \sum_i a_s^3 \hat{p}_i^4, \quad (21)$$

$$\tilde{\mathbf{p}} = \mu_r \bar{p}_i (1 + \frac{1}{6} a_s^2 \hat{p}_i^2), \quad (22)$$

with $\bar{p}_i = \frac{1}{a_s} \sin(a_s p_i)$ and $\hat{p}_i = \frac{2}{a_s} \sin(a_s p_i / 2)$. Expanding the physical solution in powers of spatial momentum yields

$$E^2(\mathbf{p}) = M_1^2 + \frac{M_1}{M_2} \mathbf{p}^2 + O(\mathbf{p}^4), \quad (23)$$

where M_1 is the rest mass, given by

$$M_1 = \frac{1}{a_t} \cosh^{-1} \left(\frac{r^2 + \mu_r m_0 r a_t - \sqrt{1 + 2\mu_r m_0 r a_t + m_0^2 \mu_r^2 a_t^2}}{r^2 - 1} \right). \quad (24)$$

The kinetic mass, M_2 is given by

$$\frac{1}{M_2} = \frac{\mu_r^2 a_t}{\sqrt{1 + 2\mu_r m_0 r a_t + m_0^2 \mu_r^2 a_t^2}} \left[\left(\frac{r^2 + \mu_r m_0 r a_t - \sqrt{1 + 2\mu_r m_0 r a_t + m_0^2 \mu_r^2 a_t^2}}{r^2 - 1} \right)^2 - 1 \right]^{-\frac{1}{2}}. \quad (25)$$

Eqs. (24) and (25) indicate that at the tree-level M_1 and M_2 do not depend on $\mathcal{O}(a_s m_q)$ terms or on the ratio of scales, ξ .

To compare these expressions with the results of other studies, the particular choice $r = 1$ was considered. In this case the lattice ghost (the unphysical solution of Eq. (20)) disappears and the dispersion relation is given by

$$4 \sinh^2 \left(\frac{Ea_t}{2} \right) = \frac{a_t^2 \tilde{\mathbf{p}}^2 + \omega^2(p)}{1 + \omega(p)}, \quad (26)$$

with

$$M_1 = \frac{1}{a_t} \log(1 + \mu_r m_0 a_t), \quad (27)$$

$$\frac{1}{2M_2} = \frac{\mu_r}{m_0(2 + \mu_r m_0 a_t)}. \quad (28)$$

where now $\mu_r = (1 + \frac{1}{2} a_t m_0)$. These expressions are consistent with those obtained in Ref. [6] for the sD34 action and in Ref. [24] for the Fermilab action on an isotropic lattice.

The free-quark dispersion relations for massless and massive quarks are shown in Figure 1. The anisotropy parameter, ξ is six for both cases. In analogy to the traditional Wilson r -parameter, the parameter s in this

action can in principle take any positive value. We chose $s = 1/8$ by eye, demanding that the energy-momentum relations do not have negative slope for $a_s |p| < \pi$. Since s parameterises a term which removes the spatial doublers and is irrelevant in the continuum limit precise tuning is not required.

IV. RESULTS

In this exploratory study the temporal rotations have been omitted which leads to an $\mathcal{O}(a_t)$ classical discretisation error. However, since a_t is small in these simulations, $a_t \sim 0.04$ fm, the effects should be under control at least when $a_t m_q < 1$. Discarding temporal rotations means the action has no clover term and in addition we have set $\mu_r = 1$. It is planned to include correction terms to remove $\mathcal{O}(a_t)$ errors in future work.

The ratio of scales is changed in a simulation by quantum corrections. Therefore the action parameter must be adjusted so that the ratio of scales measured from a physical quantity is correct. In a quenched simulation the parameters ξ_g and ξ_q in the gauge and quark actions may be independently tuned to the target anisotropy, using different physical probes. This is not the case for unquenched simulations where the anisotropy in the gauge

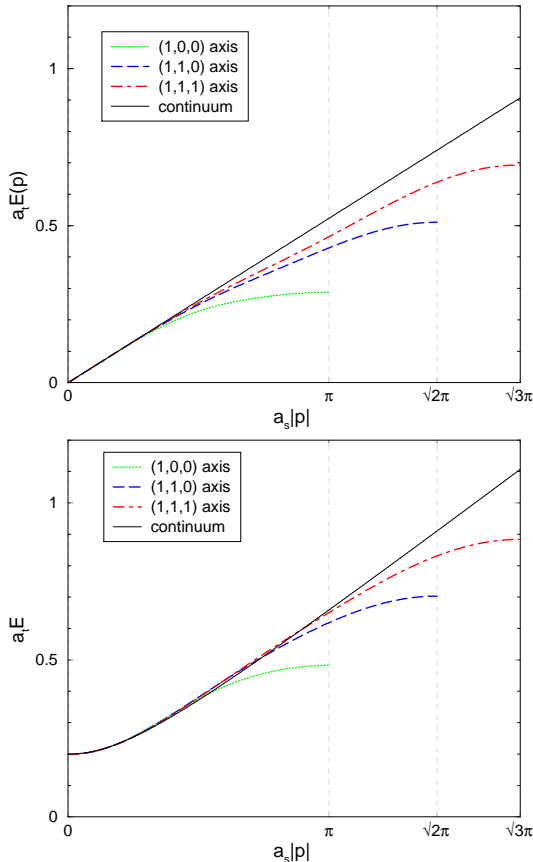


FIG. 1: The dispersion relations given by Eq. 20 with $\xi = 6$, $r = 1$ and $s = 1/8$. The top figure is the massless case while the bottom plot shows the massive case, with $a_t m_q = 0.2$.

and quark actions must be tuned simultaneously [9].

For this study an ensemble of quenched gauge configurations for which ξ_g had already been tuned was used. In this case the tuning criterion was that $\xi = 6$ when measured from the static interquark potential in different directions on the lattice. The parameter ξ_q in the fermion action must now be tuned such that its value determined from the energy momentum dispersion relation is six. At this point we introduce some terminology which makes clear the difference between ξ_q , which is a parameter in the action, and the slope of the dispersion relation which is a physical observable – usually called the speed of light, c . The target anisotropy is six. ξ_q is tuned so that the speed of light (determined from the slope of the dispersion relation) is unity.

The anisotropic action offers the possibility of precision studies of a range of phenomenologically interesting heavy quark quantities in the D , B , J/ψ and Υ sectors. For this reason it is important to understand the dependence of ξ_q on the heavy quark mass used in simulations. In particular, a contribution of $\mathcal{O}(a_s m_q)$ to the renormalised anisotropy would spoil this tuning for charm and bottom quark masses. The main result in this section is a study of the mass-dependence of the speed of light at

fixed anisotropy.

A. Simulation parameters

The gauge action used in this simulation is a two-plaquette improved action designed for precision glue-ball simulations on anisotropic lattices. A description is given in Ref. [25]. The construction of the fermion action is described in detail in Section II. Details of the simulation and parameter values are summarised in Table I. A broad range of quark masses was investigated, from

# gauge configurations	100
Volume	$10^3 \times 120$
a_s	0.21fm
a_s/r_0	0.4332(11)
$\xi = a_s/a_t$	6
$a_t m_q$	-0.04, 0.1, 0.2, 0.3, 0.4, 0.5, 1.0, 1.5

TABLE I: Details of the simulation.

$a_t m_q = -0.04$ which is close to the strange quark on these lattices to heavy quarks with $a_t m_q = 1.0$ and 1.5. Both degenerate and nondegenerate combinations are considered. The nondegenerate combination is made with the lightest quark and each of the heavier quarks. Note that $a_t m_q = -0.04$ corresponds to a positive quark mass since Wilson-type actions have an additive mass renormalisation. We accumulated data at spatial momenta $(0,0,0)$, $(1,0,0)$, $(1,1,0)$ and $(1,1,1)$, in units of $2\pi/a_s L$, averaging over equivalent momenta.

It is worth noting that all the gauge configurations and quark propagators used in this study were generated on Pentium IV workstations. Generating the lightest quark propagators (close to the strange quark mass) required approximately one week on a single processor. At this quark mass no exceptional configurations were seen.

B. Effective masses

The success of anisotropic lattice methods is predominantly due to the increased resolution in the temporal direction. The fineness of the lattice in this direction is particularly useful when determining heavy mass quantities whose signal to noise ratio decreases rapidly. The increase in resolution also leads to reduced statistical errors in effective masses since fits can be made to longer time ranges than is usually possible with an isotropic lattice. For the same reason, the fitted values tend to be less sensitive to fluctuations of one or two points in the chosen fit range.

In this study the effective masses were determined using single cosh fits with a χ^2 minimization algorithm. The signal to noise ratio was enhanced by using four sources, distributed across the lattice at timeslices 0, 30,

60 and 90. The average of these results was used in the effective mass fits. The statistical errors shown are calculated from 1000 bootstrap samples in each fit. Figure 2 shows four effective mass plots. The first plot is the pseudoscalar meson with degenerate quarks at the lightest mass for zero momentum and for momentum of $(1, 1, 1)$ in lattice units, $2\pi/a_s L$. The second plot is the analogous case for the degenerate combination of quarks with $a_t m_q = 1.0$. In all cases a clear plateau, over a large number of timeslices is observed. The fits to effective masses of the non-degenerate mesons are equally good and in all cases the fit range is ten or more timeslices with a χ^2 per degree of freedom (χ^2/N_{df}) ~ 1 . In

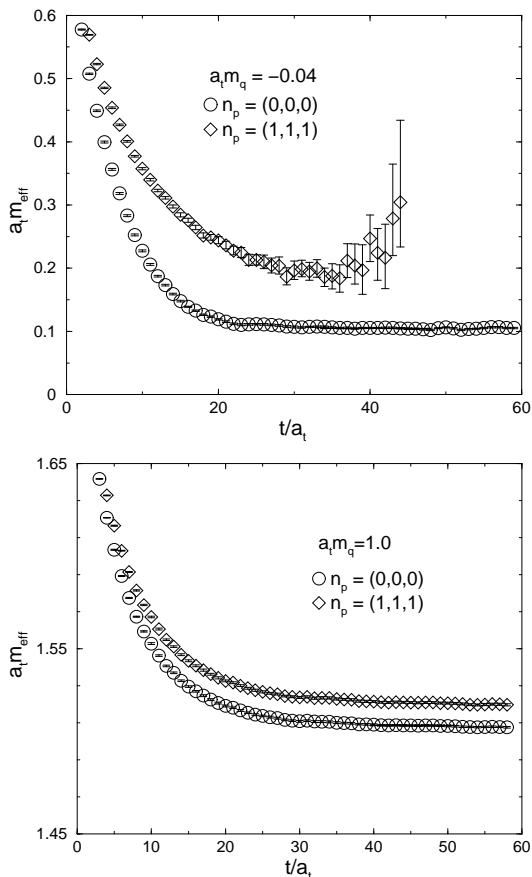


FIG. 2: Pseudoscalar meson effective mass plots. The two plots indicate that very good fits can be made for a wide range of quark masses and momenta. The top plot shows the effective mass of the lightest meson made from a degenerate combination of quarks with $a_t m_q = -0.04$ for zero momentum and for three units of momentum in lattice units. The second plot is the analogous case for $a_t m_q = 1.0$.

Figure 3 the equivalent results for vector mesons are presented. Once again, the lightest and heaviest degenerate combinations of quark masses considered are shown and very good fits are possible in both cases.

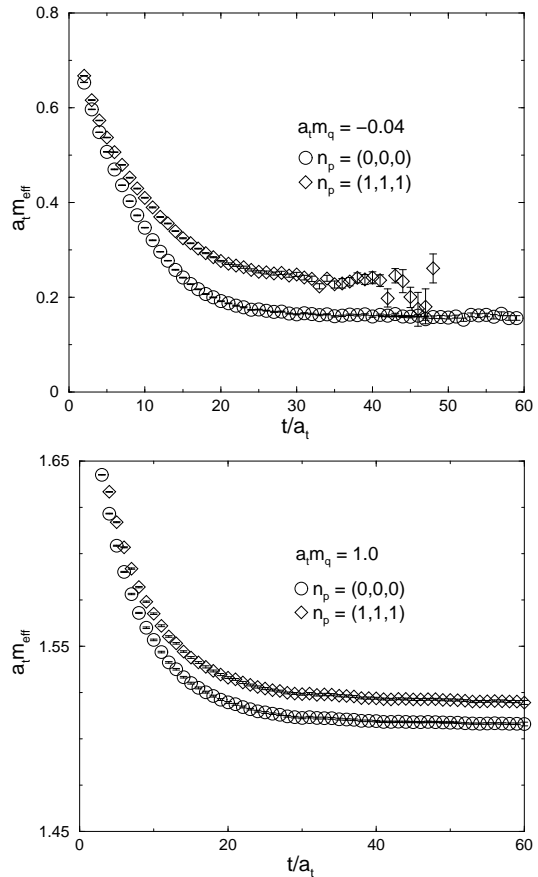


FIG. 3: Vector meson effective mass plots. As in the pseudoscalar case shown in Figure 2, good fits are achieved over a large number of timeslices for all the quark masses considered in this study. The top plot shows the lightest degenerate vector while the bottom plot shows the same result for $a_t m_q = 1.0$.

C. The renormalised anisotropy

The slope of the energy momentum dispersion relation is determined nonperturbatively and compared to the target anisotropy, $\xi = 6$. We are interested in both the precision of the determination and the deviation of the speed of light from unity. The wide range of quark masses used in this simulation ($a_t m_q = -0.04$ to $a_t m_q = 1.5$) allow us to study the mass-dependence of the renormalisation. We also examine the difference between the anisotropy determined from particles with degenerate and non-degenerate quark content.

To begin, the dispersion relation was determined for a pseudoscalar meson made from the lightest quarks in this simulation, $a_t m_q = -0.04$ and with an input anisotropy, $\xi_q = 6.0$. The value of c determined from the dispersion relation was used to determine the tuned value of the anisotropy, $\xi_q = 6.17$ and the calculation repeated. The resulting dispersion relation is shown in Figure 4. The subsequent value of c determined from this data is

1.02 ± 0.01 . This value of $\xi_q = 6.17$ was then used in sim-

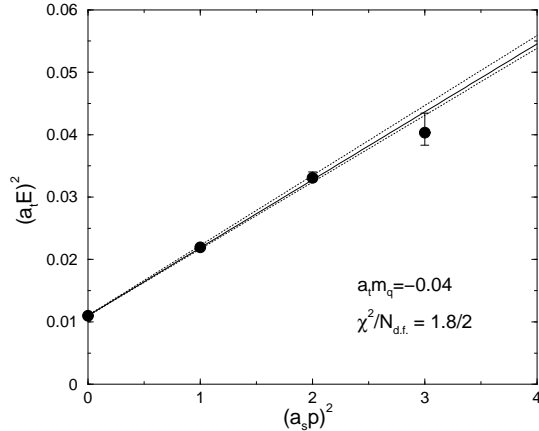


FIG. 4: The energy-momentum for the lightest degenerate meson in this simulation. The bare quark mass is $a_t m_q = -0.04$.

ulations for a range of quark masses, $0.1 \leq a_t m_q \leq 1.5$. A representative sample of the energy-momentum dispersion relations for this range of quark masses and particles is shown in Figure 5. The plot shows very good linear

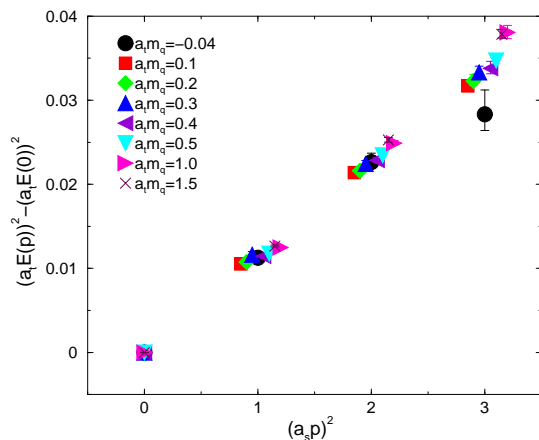


FIG. 5: The energy momentum dispersion relation for the pseudoscalar meson at all the masses simulated. The lightest point, $a_t m_q = -0.04$ is close to the strange quark while the heaviest mass is close to the bottom mass. The points have been shifted about their momentum value to make the plot easier to read.

dispersive behaviour. This relativistic dispersion relation persists for both degenerate and non-degenerate quark combinations in pseudoscalar and vector particles at all masses.

The mass-dependence of the speed of light is given by the difference in the slopes for the different masses. Figure 5 shows that this dependence is mild. The lightest mass, close to the strange quark mass, is the noisiest and the statistical errors increase with increasing momentum, as expected. It should be noted that the quark propaga-

tors used in this study are generated with point sources and the use of smearing techniques is expected to improve the signal for this and lighter quark masses. In addition the advantages of stout link gauge backgrounds [26] will be investigated in further studies.

In Tables II and III we show the speed of light determined from the slope of the dispersion relation for each mass in the simulation. The $\chi^2/N_{d.f.}$ for these fits also is shown. Results for both pseudoscalar and vector mesons are given and the ground state masses extracted in the fitting procedure described in Section IV B are listed.

$a_t m_q$	Pseudoscalar			Vector		
	$a_t M_{PS}$	c	χ^2/N_{df}	$a_t M_V$	c	χ^2/N_{df}
-0.04	0.1045_{-5}^{+5}	1.02_{-1}^{+1}	6.3/2	0.161_{-2}^{+2}	0.97_{-2}^{+2}	0.66/2
0.10	0.3831_{-4}^{+4}	0.983_{-7}^{+6}	2.8/2	0.3934_{-4}^{+4}	0.982_{-8}^{+8}	2.1/2
0.20	0.5418_{-4}^{+3}	0.995_{-7}^{+7}	0.33/2	0.5472_{-4}^{+4}	0.990_{-8}^{+8}	2.1/2
0.30	0.6887_{-4}^{+4}	1.010_{-7}^{+8}	2.4/2	0.6924_{-4}^{+4}	0.997_{-9}^{+9}	4.5/2
0.40	0.8269_{-4}^{+4}	1.022_{-5}^{+5}	0.65/2	0.8294_{-4}^{+4}	1.011_{-5}^{+5}	2.3/2
0.50	0.9569_{-4}^{+4}	1.035_{-5}^{+5}	1.3/2	0.9587_{-4}^{+4}	1.025_{-5}^{+5}	1.6/2
1.00	1.5086_{-3}^{+3}	1.069_{-5}^{+5}	1.3/2	1.5092_{-3}^{+3}	1.072_{-5}^{+5}	1.2/2
1.50	1.9428_{-3}^{+3}	1.075_{-5}^{+5}	0.081/2	1.9431_{-4}^{+3}	1.072_{-5}^{+5}	0.058/2

TABLE II: The ground state pseudoscalar and vector masses with degenerate quarks. The speed of light determined from the dispersion relation for each quark mass is shown with the associated $\chi^2/N_{d.f.}$. The errors in all cases are statistical only. The parameter, ξ_q is fixed in these simulations to 6.17, its value determined from the dispersion relation of the lightest degenerate pseudoscalar meson.

The dependence of c on the quark mass in the simulation is shown in Figures 6 and 7. The plots show the speed of light as a function of the meson mass in units of a_t for both pseudoscalars and vectors. It is important to remember that the anisotropy was tuned only once at the lightest pseudoscalar particle. The plots show good

$a_t m_q$	Pseudoscalar			Vector		
	$a_t M_{PS}$	c	χ^2/N_{df}	$a_t M_V$	c	χ^2/N_{df}
0.1	0.2610_{-6}^{+6}	0.98_{-1}^{+1}	0.23/2	0.2802_{-8}^{+8}	0.98_{-2}^{+2}	0.19/2
0.2	0.3466_{-6}^{+6}	1.01_{-2}^{+2}	0.56/2	0.3601_{-8}^{+8}	0.99_{-2}^{+2}	0.64/2
0.3	0.4254_{-7}^{+7}	1.02_{-2}^{+2}	2/2	0.4351_{-8}^{+8}	1.00_{-2}^{+2}	0.45/2
0.4	0.4987_{-7}^{+7}	1.01_{-2}^{+2}	1.5/2	0.5056_{-9}^{+8}	0.99_{-2}^{+2}	1.4/2
0.5	0.5668_{-8}^{+8}	1.02_{-2}^{+2}	1.7/2	0.5720_{-9}^{+9}	1.00_{-2}^{+2}	1.6/2
1.0	0.8521_{-10}^{+10}	1.00_{-2}^{+2}	2.6/2	0.854_{-1}^{+1}	1.02_{-3}^{+3}	0.62/2
1.5	1.074_{-1}^{+1}	1.02_{-3}^{+3}	2.1/2	1.075_{-1}^{+1}	1.01_{-4}^{+3}	1.8/2

TABLE III: The ground state masses of non-degenerate combinations of quark masses. In each case the quark mass given is combined with the lightest mass in our simulations, $a_t m_q = -0.04$. As in Table II the pseudoscalar and vector meson states are shown with the speed of light and the associated $\chi^2/N_{d.f.}$. Once again all errors are statistical only and $\xi_q = 6.17$.

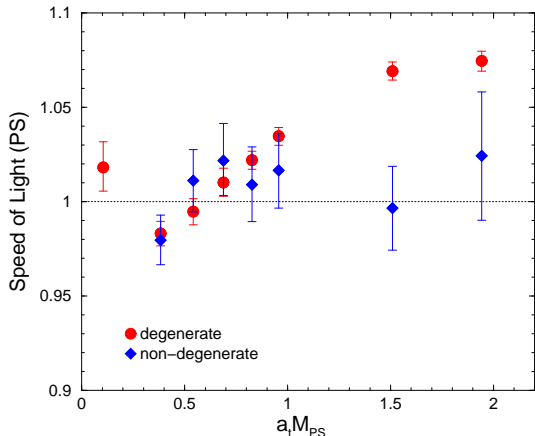


FIG. 6: The mass-dependence of the speed of light determined from the pseudoscalar (PS) dispersion relations for fixed $\xi_q = 6.17$. The plot shows mesons with both degenerate and non-degenerate quark mass combinations plotted as a function of the degenerate meson mass, in units of the temporal lattice spacing.

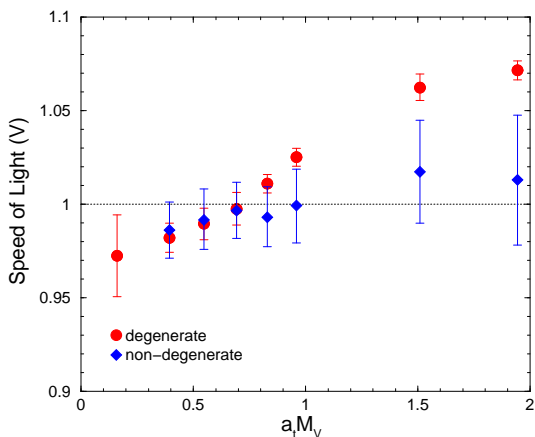


FIG. 7: The mass-dependence of the speed of light determined from the vector (V) dispersion relations with $\xi_q = 6.17$. Both degenerate and non-degenerate mass combinations are shown, plotted as a function of the degenerate vector mass as in Figure 6.

agreement between determinations of c from degenerate and non-degenerate particles up to $a_t m_q \sim 0.5$, corresponding to $a_t M_{PS} = 0.957(5)$ in Figure 6. The charm quark mass on this lattice is close to $a_t m_q = 0.2$, implying that charm physics is both computationally feasible and requires little parameter tuning at an anisotropy of six. Figures 6 and 7 also show some quark mass dependence for degenerate mesons with $a_t m_q \geq 0.5$. They also indicate that the agreement between the degenerate and non-degenerate meson physics decreases for $a_t m_q \geq 0.5$. This is not unexpected since degenerate mesons with two heavy quarks (charmonium and bottomonium) have a small Bohr radius and can suffer large discretisation effects. The non-degenerate mesons (D and B mesons) do

not have such a problem.

We have investigated this dependence by varying the parameter ξ_q in the quark action and repeating the simulations described above, for the heavy quark mass $a_t m_q = 1.0$. The dependence of the speed of light, determined from the dispersion relation, on the input anisotropy is shown in Figure 8. The value of c deter-

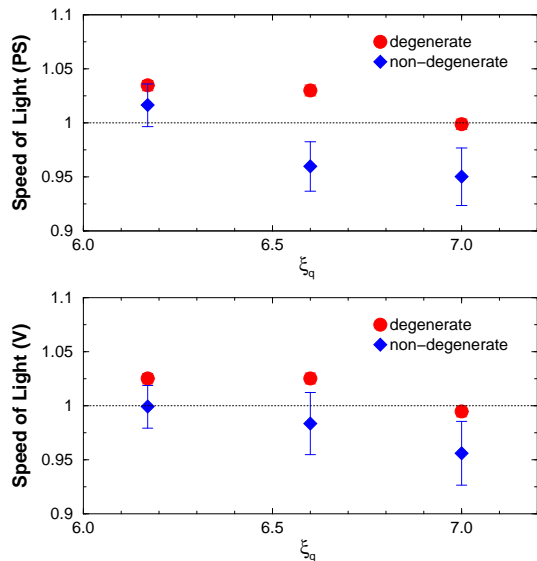


FIG. 8: The speed of light as measured from the dispersion relation as a function of the parameter, ξ_q in the action. The first plot shows the result for the pseudoscalar (PS) meson, for both degenerate and non-degenerate combinations. The second plot is the analogous result for the vector (V) mesons. In both cases the quark mass is fixed at $a_t m_q = 1.0$.

mined from the degenerate meson moves closer to its target value of unity and c determined from the non-degenerate physics moves away from this value. It is also interesting to note the agreement between determinations of c from pseudoscalar and vector particles. The tuning, described above at $a_t m_q = -0.04$ was carried out for pseudoscalars and it is reassuring that although the vector particles have larger statistical errors they nevertheless yield a consistent picture for the mass dependence of the speed of light.

V. DISCUSSION AND CONCLUSIONS

In this paper we have explored the viability of anisotropic actions for heavy quark physics. An action suitable for simulations at large anisotropies and which has no $\mathcal{O}(a_s m_q)$ errors is described. One of the main disadvantages of using anisotropic actions is the extra parameter tuning required to recover Lorentz invariance. In particular, if the ratio of scales ξ is sensitive to the quark mass in the simulation then a parameter tuning may be required for each mass. We have measured the speed of light for a range of quark masses having fixed the ratio of

scales at the strange quark, $a_t m_q = -0.04$. Only slight mass dependence (for the degenerate mesons) is found up, to $a_t m_q = 0.5$ which is heavier than the charm quark on these lattices. This implies that one measurement of the speed of light is all that is required for simulations over a large range of masses, at the percent-level of simulation. The simulations were repeated for mesons with non-degenerate quarks, using a value of ξ tuned from the degenerate meson spectrum. The results are in excellent agreement up to $a_t m_q = 0.5$. Since the charm quark on this lattice is approximately $a_t m_q = 0.2$ this work indicates that both heavy-heavy (degenerate) and heavy-light (non-degenerate) charm physics can be easily reached using an appropriately improved anisotropic action.

The results also show that heavy-light as well as heavy-heavy physics can be reliably simulated after a single tuning of ξ_q . The determination of c can be interpreted as a measure of the ratio M_1/M_2 in Eq. (23). The agreement of M_1 and M_2 for both heavy-heavy and heavy-light systems can in turn be interpreted as an absence, in this quark action, of the anomaly first discussed in Ref. [27]. This anomaly was explained in

Ref. [28] where it was pointed out that for a sufficiently accurate lattice action ($\mathcal{O}(v^4)$ in NRQCD) the discrepancies in binding energies $\delta B = B_2 - B_1$ vanishes and $I = (2\delta B_{\bar{Q}q} - (\delta B_{\bar{Q}Q} + \delta B_{\bar{q}q}))/2M_{2\bar{Q}q} = 0$ as expected. The action described in this study has this property.

This study has been carried out in the quenched approximation which is a useful laboratory in which to study mass-dependent and tuning issues at relatively low computational cost. We are currently developing algorithms for dynamical simulations with anisotropic lattices which we plan to use in a study of heavy-flavour physics.

Acknowledgments

The authors would like to thank Jimmy Juge, Colin Morningstar and Jon-Ivar Skullerud for carefully reading this manuscript. This work was funded by Enterprise-Ireland grants SC/2001/306 and SC/2001/307, by IRCSET awards RS/2002/208-7M and SC/2003/393 and under the IITAC PRTLTI initiative.

-
- [1] C. J. Morningstar and M. J. Peardon, Phys. Rev. **D60**, 034509 (1999), hep-lat/9901004.
 - [2] M. G. Alford, T. R. Klassen, and G. P. Lepage, Nucl. Phys. **B496**, 377 (1997), hep-lat/9611010.
 - [3] G. Burgio, A. Feo, M. J. Peardon, and S. M. Ryan (2003), hep-lat/0310036.
 - [4] G. Burgio, A. Feo, M. J. Peardon, and S. M. Ryan (2003), hep-lat/0309058.
 - [5] J. Harada, A. S. Kronfeld, H. Matsufuru, N. Nakajima, and T. Onogi, Phys. Rev. **D64**, 074501 (2001), hep-lat/0103026.
 - [6] S. Hashimoto and M. Okamoto, Phys. Rev. **D67**, 114503 (2003), hep-lat/0302012.
 - [7] J. Foley, A. O’Cais, M. J. Peardon, and S. M. Ryan (Trin-Lat) (2003), hep-lat/0309162.
 - [8] H. W. Hamber and C. M. Wu, Phys. Lett. **B133**, 351 (1983).
 - [9] M. Peardon, Nucl. Phys. Proc. Suppl. **109A**, 212 (2002).
 - [10] M. Okamoto et al. (CP-PACS), Phys. Rev. **D65**, 094508 (2002), hep-lat/0112020.
 - [11] X. Liao and T. Manke, Phys. Rev. **D65**, 074508 (2002), hep-lat/0111049.
 - [12] P. Chen, Phys. Rev. **D64**, 034509 (2001), hep-lat/0006019.
 - [13] R. G. Edwards, U. M. Heller, and D. G. Richards (LHP), Nucl. Phys. Proc. Suppl. **119**, 305 (2003), hep-lat/0303004.
 - [14] H. Matsufuru, J. Harada, T. Onogi, and A. Sugita, Nucl. Phys. Proc. Suppl. **119**, 601 (2003), hep-lat/0209090.
 - [15] X.-Q. Luo and Z.-H. Mei, Nucl. Phys. Proc. Suppl. **119**, 263 (2003), hep-lat/0209049.
 - [16] J. Harada, H. Matsufuru, T. Onogi, and A. Sugita, Nucl. Phys. Proc. Suppl. **111**, 282 (2002), hep-lat/0202004.
 - [17] J. Shigemitsu et al., Phys. Rev. **D66**, 074506 (2002), hep-lat/0207011.
 - [18] P. de Forcrand et al. (QCD-TARO), Nucl. Phys. Proc. Suppl. **83**, 411 (2000), hep-lat/9911001.
 - [19] T. Umeda, R. Katayama, O. Miyamura, and H. Matsufuru, Int. J. Mod. Phys. **A16**, 2215 (2001), hep-lat/0011085.
 - [20] T. R. Klassen, Nucl. Phys. **B509**, 391 (1998), hep-lat/9705025.
 - [21] T. R. Klassen, Nucl. Phys. Proc. Suppl. **73**, 918 (1999), hep-lat/9809174.
 - [22] P. Chen, X. Liao, and T. Manke, Nucl. Phys. Proc. Suppl. **94**, 342 (2001), hep-lat/0010069.
 - [23] A. Ali Khan et al. (CP-PACS), Nucl. Phys. Proc. Suppl. **94**, 325 (2001), hep-lat/0011005.
 - [24] A. X. El-Khadra, A. S. Kronfeld, and P. B. Mackenzie, Phys. Rev. **D55**, 3933 (1997), hep-lat/9604004.
 - [25] C. Morningstar and M. J. Peardon, Nucl. Phys. Proc. Suppl. **83**, 887 (2000), hep-lat/9911003.
 - [26] C. Morningstar and M. J. Peardon, Phys. Rev. **D69**, 054501 (2004), hep-lat/0311018.
 - [27] S. Collins, R. G. Edwards, U. M. Heller, and J. H. Sloan, Nucl. Phys. Proc. Suppl. **47**, 455 (1996), hep-lat/9512026.
 - [28] A. S. Kronfeld, Nucl. Phys. Proc. Suppl. **53**, 401 (1997), hep-lat/9608139.